

# Stereochemical Effect of Even–Odd Connecting Links on Supramolecular Assemblies Made of 1-Glucosamide Bolaamphiphiles

Toshimi Shimizu\* and Mitsutoshi Masuda

Contribution from the Department of Organic Materials, National Institute of Materials and Chemical Research, 1-1 Higashi, Tsukuba, Ibaraki 305, Japan

Received April 15, 1996. Revised Manuscript Received January 22, 1997<sup>⊗</sup>

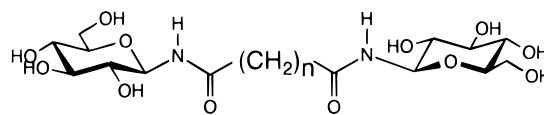
**Abstract:** Bolaamphiphiles with a 1-glucosamide-head group at each end, *N,N'*-bis( $\beta$ -D-glucopyranosyl)alkane-1, *n*-dicarboxamide [**Glc-NC(*n*)CN-Glc**, *n* = 6, 9, 10, 11, 12, 13, and 14], have been synthesized. Self-assembled supramolecular structures in water strongly depend on whether *n* is even or odd, which respectively give rise to fibrous assemblies or planar platelets as well as amorphous solids. In connection with this even–odd effect of the hydrocarbon links, internal molecular arrangements of the solid fibers were investigated using FT-IR spectroscopy, X-ray diffraction and crystal analyses, and transmission electron microscopy. The oligomethylene groups of the **Glc-NC(12)CN-Glc** pack in a monoclinic or an orthorhombic mode in the fiber. We propose a possible self-assembled model based on a monolayer sheet, which is stabilized by hydrogen-bond networks via sugar-head and amide groups.

## Introduction

Fibrous assemblies formed with synthetic amphiphiles<sup>1</sup> have recently provided a wide variety of well-defined and intriguing nano- and microstructures.<sup>2</sup> Particularly, enantiomeric amphiphiles are known to produce mirror image helices, whereas racemates only give nonhelical platelets.<sup>2j,3–6</sup> However, there has been little investigation into a stereochemical effect of even–odd hydrocarbon chains on chiral assemblies,<sup>7,8</sup> as well as their conformations in the fiber.<sup>9–11</sup>

To obtain crystalline fibers stabilized by multiple hydrogen bonds, we have synthesized a series of 1-glucosamide bolaam-

phiphiles **Glc-NC(*n*)CN-Glc** (*n* = 6, 9, 10, 11, 12, 13, and 14). Very little is known about the molecular assemblies of glucosamides<sup>12</sup> in which the polysaccharide and protein interactions are in some way combined. Furthermore, the relative orientation of the two carbonyl dipoles<sup>13</sup> should be controlled by the even or odd number of carbons in the hydrocarbon links of the bolaamphiphiles. We have recently revealed the hydrogen-bond networks in the crystal structure of **Glc-NC(11)CN-Glc**.<sup>14</sup> In this paper, the formation of chiral assemblies is investigated from the viewpoint of the even–odd effect of the connecting links. Furthermore, we report internal molecular arrangements of the self-assembled fibers.



**Glc-NC(*n*)CN-Glc** (*n* = 6, 9, 10, 11, 12, 13, and 14)

## Results and Discussion

### Observation of Crystalline Fibers by Light Microscopy.

The bolaamphiphiles **Glc-NC(*n*)CN-Glc** (*n* = 6, 9, 10, 11, 12, 13, and 14) proved to be soluble at least in hot water (up to 0.1% w/v for **Glc-NC(14)CN-Glc** at 70 °C, see Table 1). However, they are insoluble in nonpolar solvents like chloroform and hexane. When the saturated hot aqueous solutions of each bolaamphiphile were allowed to slowly cool, they afforded different types of crystalline and fibrous assemblies. Especially, the fiber-growth feature strongly depends on both the lengths of the alkylene chains and their even or odd carbon numbers.

The hexamethylene-group-spanned bolaamphiphile **Glc-NC-(6)CN-Glc** is highly soluble in water at room temperature (>50% w/v at room temperature, see Table 1). Upon successful

(11) Terech, P.; Furman, I.; Weiss, R. G. *J. Phys. Chem.* **1995**, *99*, 9558–9566.

(12) Fuhrhop, J.-H.; Koenig, J. *Membranes and Molecular Assemblies: The Synergetic Approach*; The Royal Society of Chemistry: Cambridge, 1994.

(13) Leiserowitz, L.; Tuval, M. *Acta Crystallogr., Sect. B* **1978**, *34*, 1230–1247.

(14) Masuda, M.; Shimizu, T. *Chem. Commun.* **1996**, 1057–1058.

<sup>⊗</sup> Abstract published in *Advance ACS Abstracts*, March 1, 1997.

(1) Fuhrhop, J.-H.; Helfrich, W. *Chem. Rev.* **1993**, *93*, 1565–1582.  
 (2) For recent examples of molecular rods, see: (a) Pfannmueller, B.; Welte, W. *Chem. Phys. Lipids* **1985**, *37*, 227–240. (b) Yanagawa, H.; Ogawa, Y.; Furuta, H.; Tsuno, K. *J. Am. Chem. Soc.* **1989**, *111*, 4567–4570. (c) Itoijima, Y.; Ogawa, Y.; Tsuno, K.; Handa, N.; Yanagawa, H. *Biochemistry* **1992**, *31*, 4757–4765. For molecular tubules, see: (d) Schnur, J. M. *Science* **1993**, *262*, 1669–1676. (e) Harada, A.; Li, J.; Kamachi, M. *Nature* **1993**, *364*, 516–518. (f) Thomas, B. N.; Safinya, C. R.; Plano, R. J.; Clark, N. A. *Science* **1995**, *267*, 1635–1638. (g) Kimizuka, N.; Kawasaki, T.; Hirata, K.; Kunitake, K. *J. Am. Chem. Soc.* **1995**, *117*, 6360–6361. (h) Hartgerink, J. D.; Granja, J. R.; Milligan, R. A.; Ghadiri, M. R. *J. Am. Chem. Soc.* **1996**, *118*, 43–50. (i) Shimizu, T.; Kogiso, M.; Masuda, M. *Nature* **1996**, *383*, 487–488. For molecular scrolls, see: (j) Fuhrhop, J.-H.; Demoulin, C.; Rosenberg, J.; Boettcher, C. *J. Am. Chem. Soc.* **1990**, *112*, 2827–2829. For molecular ribbons, see: (k) Shimizu, T.; Mori, M.; Minamikawa, H.; Hato, M. *J. Chem. Soc., Chem. Commun.* **1990**, 183–185. (l) Imae, T.; Takahashi, Y.; Muramatsu, H. *J. Am. Chem. Soc.* **1992**, *114*, 3414–3419. (m) Shimizu, T.; Hato, M. *Biochim. Biophys. Acta* **1993**, *1147*, 50–58. (n) Frankel, D. A.; O'Brien, D. F. *J. Am. Chem. Soc.* **1994**, *116*, 10057–10069. (o) Endisch, C.; Bottcher, C.; Fuhrhop, J.-H. *J. Am. Chem. Soc.* **1995**, *117*, 8273–8274.

(3) Tachibana, T.; Yoshizumi, T.; Hori, K. *Bull. Chem. Soc. Jpn.* **1979**, *52*, 34–41.

(4) Nakashima, N.; Asakuma, S.; Kunitake, T. *J. Am. Chem. Soc.* **1985**, *107*, 509–510.

(5) Fuhrhop, J.-H.; Schnieder, P.; Rosenberg, J.; Boekema, E. *J. Am. Chem. Soc.* **1987**, *109*, 3387–3390.

(6) Fuhrhop, J.-H.; Schnieder, P.; Boekema, E.; Helfrich, W. *J. Am. Chem. Soc.* **1988**, *110*, 2861–2867.

(7) Yamada, N.; Kawasaki, M. *J. Chem. Soc., Chem. Commun.* **1990**, 568–569.

(8) Yamada, N.; Okuyama, K.; Serizawa, T.; Kawasaki, M. *J. Chem. Soc., Perkin Trans. 2* **1996**, 2707–2714.

(9) Svenson, S.; Koenig, J.; Fuhrhop, J.-H. *J. Phys. Chem.* **1994**, *98*, 1022–1028.

(10) Terech, P.; Rodriguez, V.; Barnes, J. D.; McKenna, G. B. *Langmuir* **1994**, *10*, 3406–3418.

**Table 1.** Physical Properties of 1-Glucosamide Bolaamphiphiles and the Obtained Representative Morphologies of the Self-Assemblies from Saturated Aqueous Solutions

bolaamphiphile	<i>n</i>	mp (°C)	solubility in water (w/v %) <sup>a</sup>	morphology
<b>Glc-NC(6)CN-Glc</b>	6	207.5–208.3 (dec)	> 50 (at 25 °C)	needle-like
<b>Glc-NC(9)CN-Glc</b>	9	212.6–217.6 (dec)	nd <sup>b</sup>	amorphous solid
<b>Glc-NC(10)CN-Glc</b>	10	222.2–224.9 (dec)	nd <sup>b</sup>	long thin fiber or gel fiber
<b>Glc-NC(11)CN-Glc</b>	11	213.4–220.4 (dec)	0.52 (at 36 °C)	twin and platelet
<b>Glc-NC(12)CN-Glc</b>	12	220.2–224.0 (dec)	0.78 (at 36 °C)	helical fiber
<b>Glc-NC(13)CN-Glc</b>	13	226.3–227.3 (dec)	0.11 (at 50 °C)	amorphous solid
<b>Glc-NC(14)CN-Glc</b>	14	227.0–229.4 (dec)	<0.1 (at 70 °C)	“bow-tie”-like fiber or thin fiber

<sup>a</sup> Solubility was determined using constant-composition methods. <sup>b</sup> Not determined.

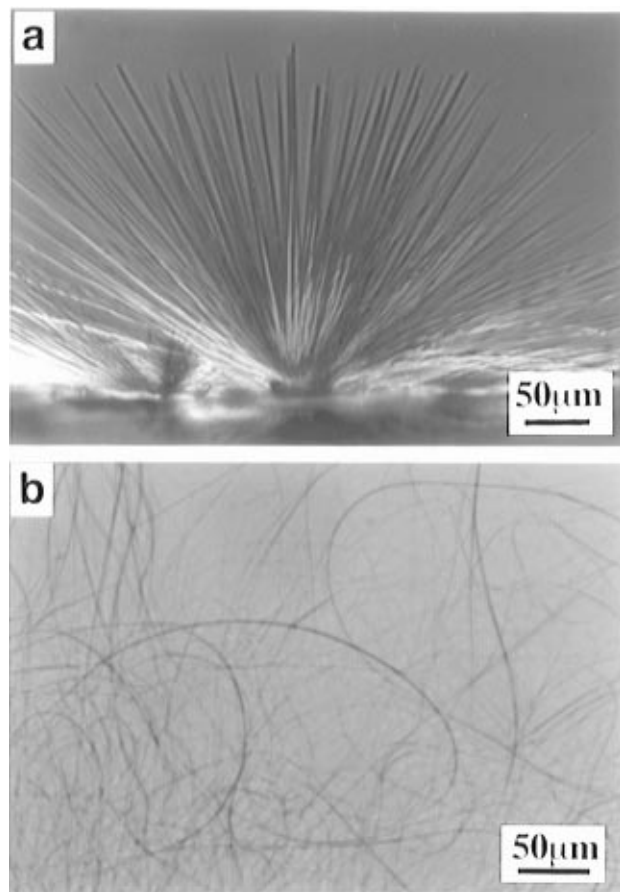


**Figure 1.** (a) Needle-like fibers made of **Glc-NC(6)CN-Glc** observed using polarized light microscopy (at 25 °C in water). (b) Flexible and thin fibrous assemblies made of **Glc-NC(10)CN-Glc** observed using polarized light microscopy (at 25 °C in water).

crystallization, it gave a common needle-like microcrystal (Figure 1a). Helical structures can be randomly seen. On the other hand, very flexible and long thin fibers, hundreds of micrometers in length, were obtained in water from the decamethylene-group-spanned bolaamphiphile **Glc-NC(10)CN-Glc** (Figure 1b). The fiber morphologies apparently resemble the noncovalently prepared organic fibers.<sup>15,16</sup> Helical morphologies can also be observed using the light microscope although they are ill-defined. The formation of these thin fibers competes with an extended hydrogelation by the same bolaamphiphiles, critically depending on the concentration, the cooling rate, and preparation method of the sample. Even if we dissolve the dehydrated hydrogels into water, no crystalline fibers can be obtained.

Elongation of the spanned alkylene chain by two methylene groups allowed the formation of right-handed twisted or helical ribbons from the bolaamphiphile **Glc-NC(12)CN-Glc**. They are of light-microscopic dimensions. Their helical pitches vary widely from 1 to 10 μm. This feature shows a good contrast to uniform helical rods and ribbons of electron-microscopic dimensions<sup>1</sup> (Figure 2a). The obtained chiral structures will come from both the amide hydrogen bond chains and the stereoselective hydrogen bonds between the glucopyranosyl head groups. Polarized light microscopy of the dried helical fibers exhibited birefringence, indicative of an extended crystalline structure (Figure 2b). The octaacetylated derivative of **Glc-NC(12)CN-Glc** did not crystallize in any nonpolar solvents but caused an extended gelation with, e.g., an ethyl acetate/*n*-hexane mixture (1/4, v/v) or tetrachloromethane. This implies that the existence of the free hydroxyl groups is responsible for the effective fiber formation in water. The maximum width of the ribbons is as large as 3 μm, and the length-to-width ratio reaches to several thousands. It is noteworthy that several bifurcated fibers were found (Figure 2c). During the course of fiber growth, two thinner separate fibers grew independently with twisting. The simultaneous occurrence of more than one crystalline form is called polymorphism in crystal engineering.<sup>17</sup> It is unknown whether the bifurcated fibers are derived from conformational or orientational polymorphism. Presumably, thermodynamic and kinetic contributions to crystal growth are complicatedly connected. As will be detailed later, the undeca-methylene-group-spanned bolaamphiphile **Glc-NC(11)CN-Glc** also tends to afford crystal polymorphism evidenced by the appearance of twin crystals. The chiral fiber formation of the 1-glucosamide bolaamphiphiles is thus delicately affected by the chemical and physical conditions in the growing media.

Dehydrated fibers made of **Glc-NC(12)CN-Glc** are somewhat fragile but extremely stable for a long term (>1 year) at temperatures lower than 220 °C in atmospheric pressure. Differential scanning calorimetry showed that **Glc-NC(12)CN-Glc** has no phase transition in water from 20 °C to 120 °C; no melting occurs up to 220 °C. Many helical microstructures have been obtained from chiral amphiphilic compounds. However, most of them are stable under limited conditions in an aqueous environment,<sup>2k,4</sup> or they form gel fibers in nonpolar solvents.<sup>18,19</sup>

We also found interesting “bow-tie”-like structures by the self-assembly of **Glc-NC(14)CN-Glc**. High-powered polarized light microscopy clearly revealed that several columnar assemblies grow and project radially from a central nucleus or associate with each other (Figure 3). However, controlled slow cooling and the subsequent slow evaporation of the saturated aqueous solution gave twisted thin fibers for **Glc-NC(14)CN-Glc** (cooling rate <0.1 °C/min).

(15) Menger, F. M.; Lee, S. J. *J. Am. Chem. Soc.* **1994**, *116*, 5987–5988.

(16) Nuckolls, C.; Katz, T. J.; Castellanos, L. *J. Am. Chem. Soc.* **1996**, *118*, 3767–3768.

(17) MacDonald, J. C.; Whitesides, G. M. *Chem. Rev.* **1994**, *94*, 2383–2420.

(18) Hidaka, H. *Colloid Surface* **1991**, *58*, 1–7.

(19) Hanabusa, K.; Yamada, M.; Kimura, M.; Shirai, H. *Angew. Chem., Int. Ed. Engl.* **1996**, *35*, 1949–1951.

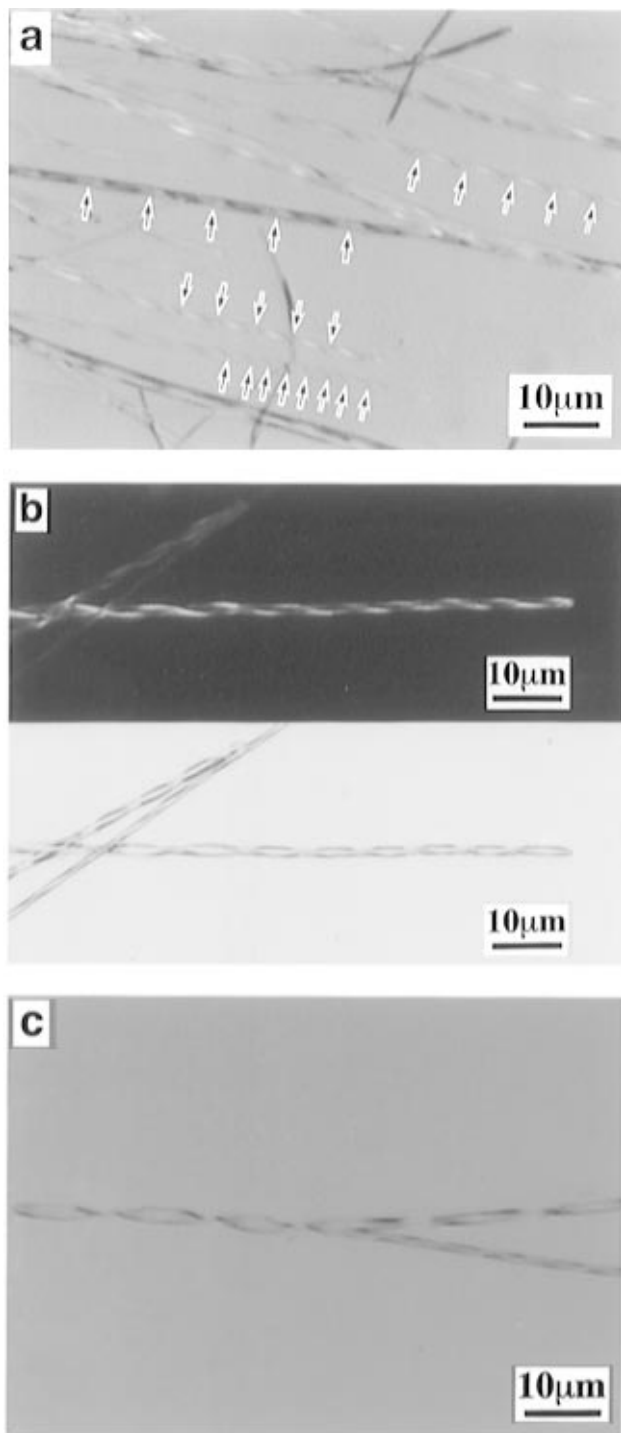


**Figure 2.** (a) A wide variety of crystalline and right-handed helical fibers made of **Glc-NC(12)CN-Glc** observed using polarized light microscopy (at 25 °C in water). Periodical structures of the fibers are denoted by arrows. (b) Polarized light micrographs of representative dehydrated and right-handed fibers from **Glc-NC(12)CN-Glc**: (upper) photographed through cross-polarized filters and (lower) through plane-polarized filters. (c) Polarized light micrograph of a bifurcated dry fiber from **Glc-NC(12)CN-Glc**.

In contrast to the fiber formation from the even-numbered bolaamphiphiles **Glc-NC(*n*)CN-Glc** ( $n = 6, 10, 12,$  and  $14$ ), amorphous solids or planar platelets were formed from the bolaamphiphiles **Glc-NC(*n*)CN-Glc** ( $n = 9, 11,$  and  $13$ ) with odd-numbered methylene carbons. Surprisingly, most of the crystals (>90%) from **Glc-NC(11)CN-Glc** exist as a twin in water. Figure 4 shows the stacked platelets with two different directions of crystal growth. The angles between the two long

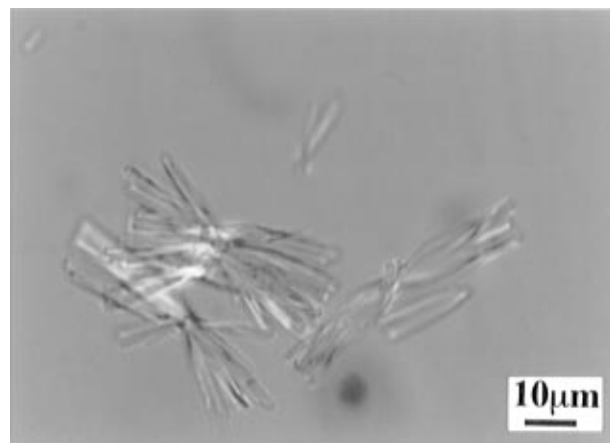


**Figure 3.** "Bow-tie"-like fibrous assemblies made of **Glc-NC(14)CN-Glc** observed using polarized light microscopy (at 25 °C in water). This 1-glucosamide bolaamphiphile also forms long thin fibers by careful cooling of the saturated aqueous solution.

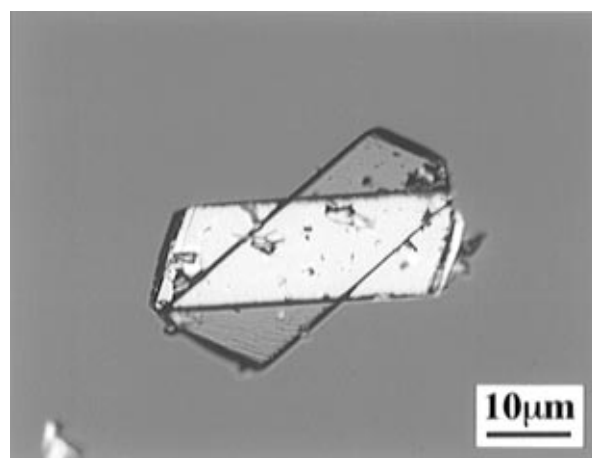


**Figure 4.** Representative twin crystal formed with **Glc-NC(11)CN-Glc**. Successfully obtained single crystal was subjected to X-ray crystal analysis.<sup>14</sup>

axes of each platelet vary from 10° to 30°. X-ray crystallographic analysis of the single crystal revealed a hydrogen-bond-assisted layered structure.<sup>14</sup> In the solid state, the alkylene chains are arranged in an antiparallel pleated sheet. In addition, cooperative and complementary hydrogen-bonding networks stabilize the amphiphilic crystal structure via the sugar hydroxyl and the amide groups.

**Even–Odd Effect of Connecting Links.** Table 1 summarizes the light microscopic morphologies of the supramolecular structures from a series of 1-glucosamide bolaamphiphiles. One notices an interesting tendency (Table 1); the fibrous assemblies are formed when  $n$  is even, and platelets or amorphous solids are formed when  $n$  is odd. On the other hand, monoheaded enantiomeric amphiphiles are known to form chiral fibers, whereas racemates precipitate as platelets without any curvature.<sup>2j,3–6</sup> These reports indicate that the chirality of the amphiphiles strongly affect the curvature of the generated molecular assemblies. However, in the present bolaamphiphile, the stereochemistry of two terminal sugar-head groups are of the same D-configuration. Therefore, the above tendency shows the first example of this stereochemical effect by the even–odd connecting links on the supramolecular assemblies.

The crystal packing mode of **Glc-NC(11)CN-Glc**<sup>14</sup> provides valuable information about the networks and directions of the amide hydrogen bond chains (Figure 5a). The molecules within each layer are identical and related by translations, whereas the

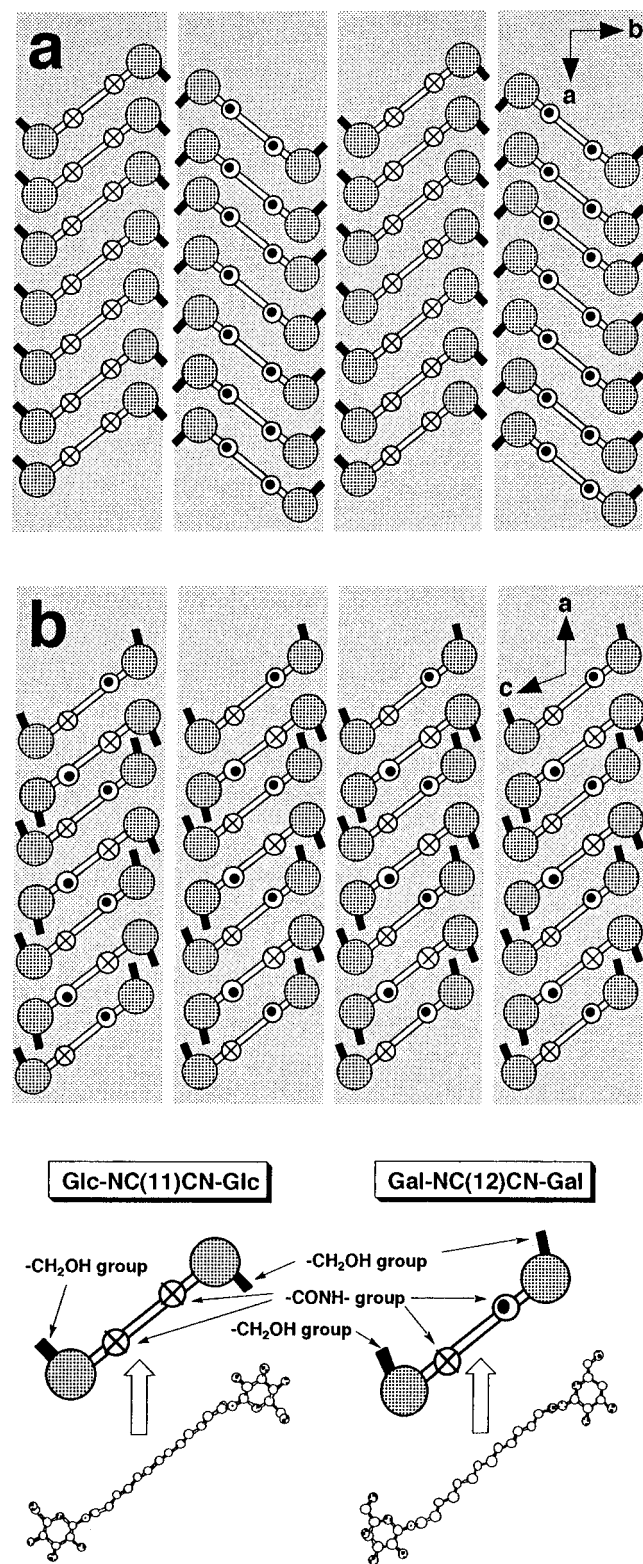


**Figure 5.** Crystal packing patterns of (a) **Glc-NC(11)CN-Glc**<sup>14</sup> and (b) **Gal-NC(12)CN-Gal**,<sup>20</sup> viewed along the *c*-axis. The amide hydrogen bond chains run roughly along the *c*-axis. The symbols (⊗) and (⊙) represent the amide group in which the carbonyl oxygen atom is placed below and above the plane, respectively.

molecules in successive layers have opposite orientations. The layers are arranged in a pleated sheet. The directions of the amide hydrogen bond chains are the same within the individual layer and alternate between the layers. As a consequence, the macrodipoles of the layers compensate each other. Namely, when *n* is odd, the generated macrodipoles allow the layers to extend through the planes that are perpendicular to the chain

axes of the amide hydrogen bonds. Although no crystal structures are yet available for the even-numbered 1-glucosamide bolaamphiphiles, we have recently succeeded in the X-ray single-crystal analysis of an even-numbered 1-D-galactosamide derivative, *N,N'*-bis( $\beta$ -D-galactopyranosyl)dodecane-1,12-dicarboxamide [**Gal-NC(12)CN-Gal**].<sup>20</sup> If one does not take into account the difference in the diastereomeric structures, these two crystal structures will enable us to make reasonable discussions about the even-odd effect of the connecting links. The **Gal-NC(12)CN-Gal** molecules are found to pack in a parallel sheet (Figure 5b). In addition, the connecting oligomethylene chains take an *all-trans* zigzag conformation. The two carbonyl dipoles compensate each other within a molecule, and eventually the antiparallel linear chains of hydrogen bonds are formed in each molecule and within layer. Thus, the even-odd effect of the hydrocarbon links would partly reflect the difference in the relative orientation of the two carbonyl dipoles within a molecule.

**Characterization of Fiber Structures.** As already mentioned, we obtained three dehydrated crystalline fibers for **Glc-NC(*n*)CN-Glc** (*n* = 6, 12, and 14) and one lyophilized gel fiber for **Glc-NC(10)CN-Glc**. Furthermore, we have a single crystal for **Glc-NC(11)CN-Glc** and crystalline powders for **Glc-NC(*n*)CN-Glc** (*n* = 9 and 13). Although the crystallinities of the obtained self-assemblies are not uniform, both a Fourier-transform infrared spectroscopy (FT-IR) and powder X-ray diffraction studies should be useful in the establishment of the internal molecular arrangements of the fibrous assemblies. Therefore, we focused our attention upon the influence of the even-odd numbers of the methylene chains on the conformation and their packing.

**FT-IR Spectroscopy.** FT-IR spectroscopy for the dehydrated fibers from **Glc-NC(*n*)CN-Glc** (*n* = 10, 12, and 14) showed the appearance of the amide I and II bands at 1657–1659 and 1534–1551  $\text{cm}^{-1}$ , respectively (see Table 2). This finding strongly supports the existence of the amide hydrogen bonds. In addition, the peak frequencies of the amide I and II bands clearly show an even-odd effect for the chain length (*n*) (*n*  $\geq$  11) (Figure 6). The absorption frequencies of the C=O stretching band (amide I) should decrease with the hydrogen-bond formation, whereas those of the N–H deformation band (amide II) should increase. Therefore, it can be at least said that the **Glc-NC(*n*)CN-Glc** molecules (*n* = 12 and 14) form weaker hydrogen bonding between the amide groups than the odd-numbered derivatives (*n* = 11 and 13). A similar even-odd effect on the amide absorption bands has been reported for the cast films of azobenzene containing amphiphiles.<sup>8</sup>

**X-ray Diffraction.** By taking advantage of the crystallinity, we carried out low- and wide-angle powder X-ray diffraction experiments with the dehydrated fibers and crystals from the 1-glucosamide bolaamphiphiles. The observed characteristic diffraction data are also listed in Table 2. The low-angle diffraction comes from the characteristic lattice repeat, i.e., the long-range ordering of the bolaamphiphiles, whereas the wide-angle region is indicative of the hydrocarbon chain packing, i.e., the short-range ordering.

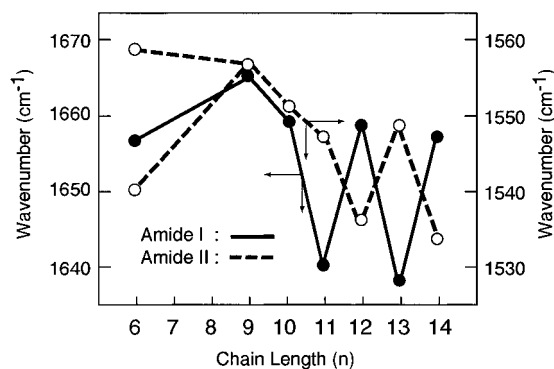
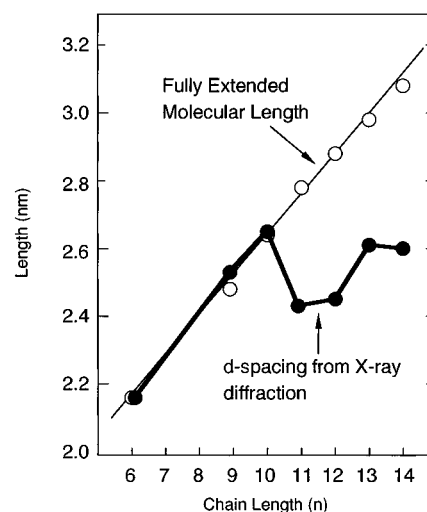
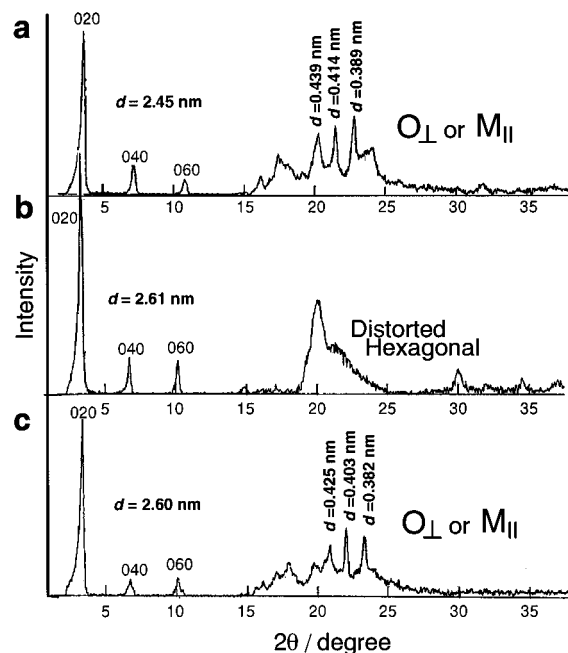
Representative X-ray diffraction diagrams are shown in Figure 7 for the dehydrated fibers from **Glc-NC(*n*)CN-Glc** (*n* = 12, 13, and 14). The diffraction patterns of all the samples show Bragg peaks typical of crystalline or solid systems. Each low-angle region is characterized by one sharp and two narrow reflections. By using Bragg's equation, we deduced the characteristic 2.45-, 2.61-, and 2.60-nm long spacing for the fibers from **Glc-NC(*n*)CN-Glc** (*n* = 12, 13, and 14, respec-

(20) Masuda, M.; Shimizu, T. Unpublished results.

**Table 2.** FT-IR Spectroscopic Absorption Bands and X-ray Diffraction Data for the Self-Assemblies from 1-Glucosamide Bolaamphiphiles

bolaamphiphile	sample nature	FT-IR data (cm <sup>-1</sup> )		representative X-ray diffraction (nm)				
		amide I	amide II	long spacing	short spacing			packing mode
<b>Glc-NC(6)CN-Glc</b>	dehydrated fiber	1657	1559, 1540	2.16	0.447	0.418	0.37	O <sub>L</sub> or M <sub>II</sub>
<b>Glc-NC(9)CN-Glc</b>	crystalline powder	1665	1557	2.52	0.448	0.400	0.38	T <sub>II</sub>
<b>Glc-NC(10)CN-Glc</b>	dehydrated fiber	1659	1551	2.67	<i>b</i>	<i>b</i>	<i>b</i>	Dh <sup>a</sup>
<b>Glc-NC(11)CN-Glc</b>	crystalline powder	1640	1547	2.43	0.465	0.401	0.382	T <sub>II</sub>
<b>Glc-NC(12)CN-Glc</b>	dehydrated fiber	1659	1536	2.45	0.439	0.414	0.389	O <sub>L</sub> or M <sub>II</sub>
<b>Glc-NC(13)CN-Glc</b>	crystalline powder	1638	1549	2.61	<i>b</i>	<i>b</i>	<i>b</i>	Dh <sup>a</sup>
<b>Glc-NC(14)CN-Glc</b>	dehydrated fiber	1657	1534	2.60	0.425	0.403	0.38	O <sub>L</sub> or M <sub>II</sub>

<sup>a</sup> Distorted hexagonal. <sup>b</sup> No well-defined peaks were obtained because of the broadening.

**Figure 6.** FT-IR peak frequencies of amide I and II bands as a function of the chain length (*n*) of the 1-glucosamide bolaamphiphiles.**Figure 8.** Dependence of both the fully extended molecular lengths (*L*) and the *d*-spacings obtained from X-ray diffraction on the chain length (*n*) of the 1-glucosamide bolaamphiphiles.**Figure 7.** Powder X-ray diffraction diagrams of the dehydrated fibers from **Glc-NC(*n*)CN-Glc** [(a) *n* = 12, (b) *n* = 13, and (c) *n* = 14]. For reference, the inserts represent related arrangements of the oligomethylene chains.

tively). The long-range ordering for the assemblies from **Glc-NC(*n*)CN-Glc** (*n* = 6, 9, 10, and 11) was also similarly evaluated and summarized in Table 2. The obtained 2.43-nm *d*-spacing from **Glc-NC(11)CN-Glc** corresponds to the half size of the *b*-axis in the crystal cell.<sup>14</sup> This implies that the high and sharp reflections at about  $\approx 3.5^\circ$  ( $2\theta$ ) will come from the (020) plane. Figure 8 compares both the obtained *d*-spacings and the estimated lengths (*L*) of the fully extended molecules as a function of the chain length (*n*). The dependence of the *d*-spacings significantly deviates from a linear relationship between *L* and *n* ( $n \geq 11$ ). It is noteworthy that the *d*-spacings alternate between the even and odd numbers for the higher

methylene carbons ( $n \geq 11$ ). Taking into account an *all-trans* conformation in all cases, one can presume that bolaamphiphiles with a longer alkyl chain are arranged by inclining against a layer plane within the fiber. In other words, the obtained *d*-spacings correspond to either a thickness of a molecular sheet or a diameter of a micellar rod. Within this monolayer sheet or the micellar rod, the interlipid interval via the amide hydrogen bonds would retain a certain backbone–backbone distance (0.47–0.49 nm).<sup>13</sup>

In the wide-angle region, we observed remarkable differences in the molecular packing of the hydrocarbon chains for the even- and odd-numbered bolaamphiphiles (Table 2). Sharp reflections appeared at  $2\theta$  corresponding to *d* = 0.465, 0.401, and 0.382 nm in the diffraction diagram for the crystalline **Glc-NC(11)CN-Glc**. The occurrence of these three peaks corresponds to a triclinic packing of the hydrocarbon chains, designated by *T*//.<sup>21</sup> The same packing mode was assumed for **Glc-NC(9)CN-Glc** based on the similarity of the peak occurrence. On the other hand, we found another series of reflections, i.e., three characteristic reflections at  $2\theta$  corresponding to *d* = 0.439, 0.414, and 0.389 nm for the dehydrated fiber of **Glc-NC(12)CN-Glc** (Figure 7a). By comparison with the X-ray diffraction data of related long-chain amphiphiles,<sup>22–24</sup> we can propose an orthorhombic (O<sub>L</sub>) or a monoclinic (M<sub>II</sub>) hydrocarbon-chain packing for this fiber. Similar results were obtained for the fibers from **Glc-NC(*n*)CN-Glc** (*n* = 6 and 14) (see Table 2 and Figure 7c). In contrast, the broad and complicated

(21) Vand, V. *Acta Crystallogr.* **1951**, 4, 104–105.

(22) Goto, M. *Jpn. Oil Chem. Soc. (YUKAGAKU)* **1970**, 19, 583–599, and references cited therein.

(23) Goto, M.; Asada, E. *Bull. Chem. Soc. Jpn.* **1978**, 51, 2456–2459.

(24) Garti, N.; Sato, K. *Crystallization and Polymorphism of Fats and Fatty Acids*; Marcel Dekker: 1988.

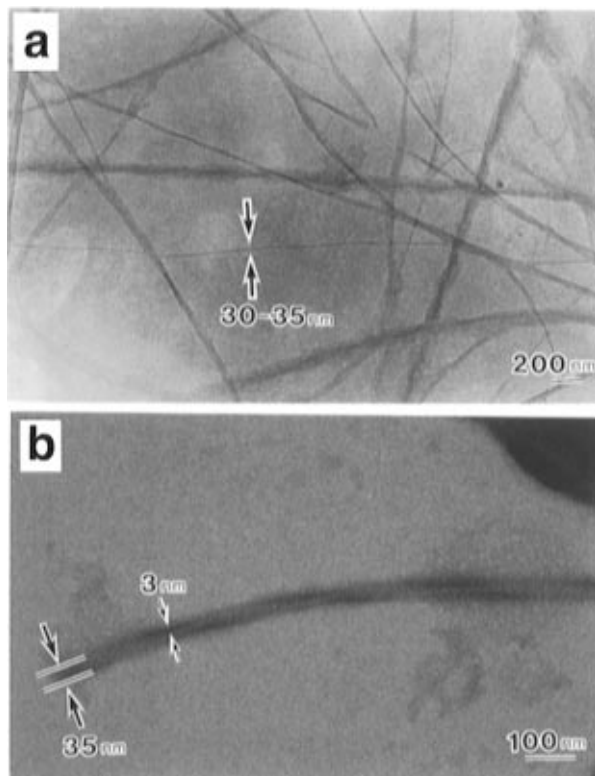


**Figure 9.** Transmission electron micrographs of (a) unstained fibrous assemblies made of **Glc-NC(12)CN-Glc** and (b) negatively stained fibers with 2%-phosphotungstic acid. When the width of the unstained fiber is greater than 50 nm in length, helical morphologies can be detected.

reflections indicate the existence of a disordered hexagonal packing of the methylene chains for **Glc-NC(*n*)CN-Glc** ( $n = 10$  and  $13$ ) (see Table 2 and Figure 7b). The above results demonstrate that the hydrocarbon-chain packing within the fibers from **Glc-NC(*n*)CN-Glc** ( $n = 10, 12$  and  $14$ ) is different from that of the odd-numbered bolaamphiphiles ( $n = 9$  and  $11$ ).

**Electron Microscopy.** Polarized and phase-contrast light microscopies demonstrate that the crystalline fibers formed with **Glc-NC(12)CN-Glc** retain a characteristic helical microstructure. To explore the fine fiber structures, we carried out transmission electron microscopy (TEM) for the unstained fibers. The TEM clearly shows that the thinnest width of the fiber is about 30–35 nm (Figure 9a). We found a wide variety of fibers with nonuniform widths. The growth of a unit fiber into higher ordered assemblies appears to be uncontrollable. Helical morphologies are visible for the fibers with more than a 50-nm width. The length of the fully extended **Glc-NC(12)CN-Glc** molecule is approximately 2.9 nm based on molecular modeling (Figure 8). Therefore, the observed minimum width ( $\approx 30$  nm) of the fiber corresponds to the lengths of ten extended bolaamphiphiles. Negatively stained fibers proved to retain a helical morphology. The width of the thinnest specimen is about 35 nm (Figure 9b). A monolayered helical sheet structure can be supported by the appearance of dark helical edges, whose width is about 3 nm.

**Internal Molecular Arrangements of Fibers.** We carried out an FT-IR spectroscopy, X-ray diffraction study, and electron microscopy for the dehydrated fibers from the 1-glucosamide bolaamphiphiles. Consequently, we could collect several evidence to depict a possible self-assembling model based on the monolayered sheet structure. It is illustrated in Figure 10 for the fiber made of **Glc-NC(12)CN-Glc**. The 2.45-nm long spacing represents the width of the monolayer sheet. The

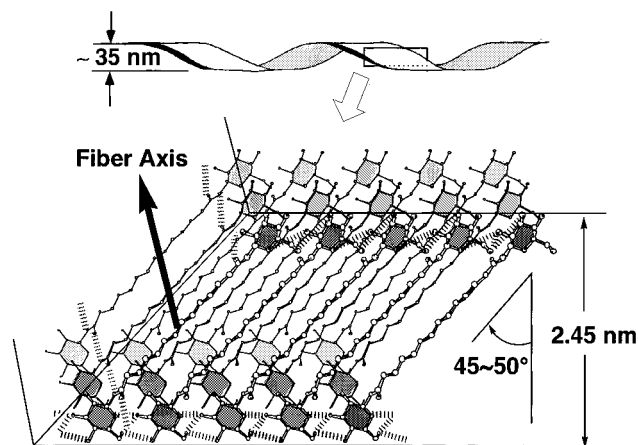


**Figure 10.** A possible self-assembling model based on the monolayered chiral sheet of **Glc-NC(12)CN-Glc**. The hydrogen-bond networks between the sugar-head groups are tentatively depicted by reference to those in the crystal structure<sup>14</sup> of **Glc-NC(11)CN-Glc**.

bolaamphiphiles pack side by side to form the monolayer sheet. In addition, the molecules are tilting their hydrocarbon chains against the monolayer plane. The inclination is estimated to be 45–50° with respect to the plane normal. Their packing modes in the fibers should be orthorhombic or monoclinic. As for the intermolecular hydrogen bonds between the glucopyranosyl groups, we can refer to the crystal structure of **Glc-NC(11)CN-Glc**.<sup>14</sup> According to the analysis, the atomic distances between the hydroxyl oxygen at the 3- and 5-positions (2.830 Å), at the 3- and 6-positions (2.911 Å), and at the 4- and 6-positions (2.957 Å) are indicative of the existence of intralayer and intermolecular hydrogen bonds. Similar hydrogen bonds between the sugar-head groups could also be formed in the fibers, contributing to the formation of the characteristic helical fibers on the light microscopic scale.

Similarly, the combined attraction forces of the intermolecular hydrogen bonds and hydrophobic interactions promote additional association between the monolayered micellar rods. Fiber formation via this self-assembling process is exemplified by the  $\alpha$ -amino- $\omega$ -lysine bolaamphiphile,<sup>25</sup> arborols,<sup>26</sup> and phospholipids with a nucleotide-head group.<sup>2b,2c</sup>

In summary, the noncovalent construction of solid-like fibrous assemblies by novel 1-glucosamide bolaamphiphiles have been described. The chiral–achiral effect of the even and odd connecting links on the supramolecular structures is reported for the first time.

## Experimental Section

**General Methods.** <sup>1</sup>H-NMR spectra were recorded with a Bruker AMX 300 spectrometer by using the 3-(trimethylsilyl)propionic acid-*d*<sub>4</sub> sodium salt as an internal standard for the aqueous solutions. For the FT-IR and DSC measurements, a JASCO FT/IR-5300 spectrometer (resolution = 4 cm<sup>-1</sup>) and a Seiko Denshi SSC 560U calorimeter (scanning rate = 1.0°/min) were used, respectively.

**Synthesis of 1-D-Glucosamide Bolaamphiphiles.** The 1-D-glucosamide bolaamphiphiles **Glc-NC(*n*)CN-Glc** ( $n = 6, 9, 10, 11, 12, 13,$  and  $14$ ) were synthesized according to the following scheme. In a typical synthesis, a commercially available acetobromo- $\alpha$ -D-glucose was treated with sodium azide to give a crystalline  $\beta$ -1-azide derivative of the tetraacetylated glucose. The stereochemical purity of this azide was checked by <sup>1</sup>H-NMR spectra. It clearly revealed the presence of

(25) Fuhrhop, J.-H.; Spiroski, D.; Boettcher, C. *J. Am. Chem. Soc.* **1993**, *115*, 1600–1601.

(26) Newkome, G. R.; Baker, G. R.; Arai, S.; Saunders, M. J.; Russo, P. S.; Theriot, K. J.; Moorefield, N.; Rogers, L. E.; Miller, J. E.; Lieux, T. R.; Murray, M. E.; Philips, B.; Pascal, L. *J. Am. Chem. Soc.* **1990**, *112*, 8458–8465.

only one doublet with  $J = \approx 8.6$  Hz for the anomeric proton, indicating a 100%  $\beta$ -glycosidic linkage. This compound was hydrogenated in the presence of platinum oxide into a  $\beta$ -1-amino derivative, which was directly condensed with a corresponding long-chain  $\alpha,\omega$ -dicarboxylic acid chloride (20–60% yield). Purification of the octaacetylated derivatives by silica-gel column chromatography (eluent: chloroform/methanol = 20/1, *v/v*) and the succeeding deacetylation produced the raw bolaamphiphiles. Purification by silica-gel column chromatography (eluent: chloroform/methanol/water = 6/4/1, *v/v*) affords the requisite 1-D-glucosamide bolaamphiphiles. The 100%  $\beta$ -configuration of each bolaamphiphile was also confirmed by an anomer proton signal in  $^1\text{H-NMR}$  spectra. The purity was confirmed by thin-layer chromatography on silica gel plates (Merck F60 254) and MALD-TOFMS (Shimadzu/Kratos KOMPACT MALDI III) using sinapinic acid as a matrix.  $^1\text{H NMR}$  of **Glc-NC(12)CN-Glc** (300 MHz,  $\text{D}_2\text{O}$ , 83 °C):  $\delta$  4.95 (d,  $J = 9.1$  Hz, 2H, H-1), 3.88 (dd,  $J = 11.9$  and 2.0 Hz, 2H, H-6b), 3.72 (dd,  $J = 11.9$  and 5.2 Hz, 2H, H-6a), 3.55 (dd,  $J = 9.3$  and 9.1 Hz, 2H, H-3), 3.50 (m,  $J = 8.8$ , 5.2, and 2.0 Hz, 2H, H-5), 3.42 (dd,  $J = 9.3$  and 8.8 Hz, 2H, H-4), 3.40 (dd,  $J = 9.1$  and 9.1 Hz, 2H, H-2), 2.32 (t,  $J = 7.3$  and 7.4 Hz, 4H,  $-\text{CH}_2\text{CONH}-$ ), 1.61 (m, 4H,  $-\text{CH}_2\text{CH}_2\text{-CONH}$ ), 1.30 (m, 16H,  $-\text{CH}_2-$ ).  $[\alpha]^{25}_{\text{D}} = -15.2$  (*c* 0.303). Anal. Calcd for  $\text{C}_{26}\text{H}_{48}\text{N}_2\text{O}_{12}$ : C, 53.78; H, 8.33; N, 4.82. Found: C, 53.90, H, 8.33; N, 4.77. In the same way, the other purified bolaamphiphiles gave satisfactory  $^1\text{H-NMR}$  spectra and elemental analyses.

**Preparation of Solid-like Fibers and Light Microscopy.** The crystalline fibrous assemblies were formed by heating the saturated aqueous solutions to 100 °C and slowly cooling them to room temperature. The cooling rate was controlled within 1–2 °C/min, and the aqueous solution was slowly evaporated. For the light microscopy measurement, a drop of the dispersion containing the fibrous assemblies was placed on the slide glass, covered with a coverslip, and sealed at the edges with adhesive tape. The samples were examined using a phase-contrast light microscope (Olympus BX50, UPlanF1 20X, 40X, 100X objective) and polarized light microscope (Olympus BX50, LMPlanF1, 20X, 50X objective). The micrograph images were recorded either by a highly sensitive camera with automatic exposure adjustments (Olympus PM30) or a 3-CCD Color Video Camera (Olympus CS520MD) equipped with variable gain and offset adjustments and monitored on a 21-in. color monitor (Ikegami TM2150M). The picture images were stored using a magneto-optical disk-drive

instrument (TEAC MV-70) as a freeze picture and printed out using a Color Video Copy Processor (Mitsubishi CP-2000). The overall magnification on the picture monitor was from 1000X to 5500X.

**Transmission Electron Microscopy.** The unstained specimen for the electron microscopy was prepared by supplying a drop of supernatant in a fiber-containing dispersion onto a grid coated with a conductive osmium plasma film.<sup>27,28</sup> The grids were blotted off with filter paper and dried in air. Negatively stained samples were prepared using phosphotungstic acid (2%). A small amount of staining solution was applied on the same carbon films and immediately drained off. The transmission electron microscope was a Zeiss CEM-902 with an accelerating voltage of 80 KV. The observation was carried out at room temperature. The magnification was from 5000X to 130 000X.

**X-ray Diffraction.** Dehydrated samples of the fibrous assemblies were prepared by the isolation of the fibers and their subsequent lyophilization. The dried fibers were cautiously powdered. All powder spectra were taken on a Rigaku RAD-C powder diffractometer using graphite-monochromated  $\text{CuK}\alpha$  radiation (40 KV, 30 mA). The spectra were measured at room temperature between 1° and 41° in the  $2\theta/\theta$ -scan mode with steps of 0.01° in  $2\theta$  and 0.6-s measurement time per step.

**Acknowledgment.** This work was partly supported by the New Energy and Industrial Technology Development Organization (Advanced Industrial Technology Research, “Synthesis of Polymer Objects”). We thank colleagues Dr. K. Yase for the skillful electron microscopy and Dr. M. Goto for her valuable discussion concerning the X-ray diffraction study.

**Supporting Information Available:** Graphical data of the molecular structures and the crystal packing of the **Glc-NC-(11)CN-Glc**, **Gal-NC(10)CN-Gal**, and **Gal-NC(12)CN-Gal** molecules (6 pages). See any current masthead page for ordering and Internet access instructions.

JA961226Y

(27) Tanaka, A. *J. Electron Microsc.* **1994**, *43*, 177–182.

(28) Yase, K.; Horiuchi, S.; Kyotani, M.; Yamamoto, K.; Yaguchi, A.; Futaesaku, Y.; Suwa, T.; Kakimoto, M.; Imai, Y. *Jpn. J. Appl. Phys.* **1996**, *35*, L657–L660.